

COASTAL MESOSCALE CONVECTIVE SYSTEMS
OF THE AUSTRALIAN MONSOON

by Dean D. Churchill* and Robert A. Houze, Jr.
Department of Atmospheric Sciences, AK-40
University of Washington
Seattle, Washington 98195

1. INTRODUCTION

During January and February 1987, The Australian Mesoscale Experiment (AMEX) was conducted to document the meso- and synoptic-scale meteorology of the Australian summer monsoon. We used radar reflectivity data collected from the land-based radar located near Darwin, Australia, to describe the structure of mesoscale precipitating systems and relate their characteristics to the synoptic scale environment.

2. SOURCES OF DATA

Weather radar data, upper-air soundings, and pluviograph data at Darwin were used in this study along with Japanese geosynchronous satellite (GMS-1) imagery. The radar characteristics are shown in Table 1.

Table 1: Characteristics of the WF44 weather radar at Darwin, Australia

Wavelength	10	cm
Peak power	650	kW
Pulse length	450	m
Minimum detectable reflectivity	15	dBZ
Pulse repetition frequency	275	Hz
Beam width	3	deg
Maximum recorded range	256	km
Recorded gate spacing	2	km
Recorded azimuth spacing	1	deg

Other details of sources of data are provided by Churchill and Houze (1991). The radar obtained low-elevation scans continuously during the period of 12 January - 15 February 1987, and these data were digitized into 6 levels of radar reflectivity and stored on tape once every 10 min. We mapped the radar reflectivities into Cartesian maps, with a horizontal resolution of 2 km, and estimated rainfall rates at each grid point by assigning a fixed rainfall rate to each of the 6 levels of radar reflectivity. We partitioned the reflectivities into stratiform and convective components using the objective technique of Churchill and Houze (1984). We examined all mesoscale systems seen on Darwin radar, features that were at least 100 km in maximum diameter, sometime during their lifetime, and which lasted at least 1 h.

*Current affiliation: Rosenstiel School of Marine and Atmospheric Science, University of Miami
Miami, Florida

Upper-air soundings were obtained every 6 h at Darwin during AMEX, as well as at 13 other locations in northern Australia. The soundings were obtained from 2300 UTC 9 January through 2300 UTC 14 February 1987. These data were provided to us by the Bureau of Meteorology Research Centre, Melbourne Australia. Infrared satellite images obtained by the GMS-1 geosynchronous satellite at 3-hourly intervals during EMEX were obtained from NOAA/NESDIS/RAMM Branch, Dept. of Atmospheric Sciences, Colorado State University; Ft. Collins, CO 80523. These images were re-navigated to a Cartesian grid with horizontal resolution 0.1° of latitude, to facilitate comparison with the gridded radar data.

3. RESULTS

3.1 Period 1

The weather of northern Australia during January - February 1987 was characterized by synoptic-scale periods of warm, moist northwesterly flow from the ocean, with frequent precipitation, punctuated by synoptic-scale periods of dry weather. The synoptic-scale variations, indicated by a series of 850 mb streamline charts (not shown) during 11 January to 14 February 1987 defined 7 time periods, within each of which the synoptic-scale conditions and the mesoscale structures were reasonably uniform. These time periods and the general synoptic conditions are listed in Table 2.

Table 2: Synoptic periods (P) near Darwin during EMEX. The start and stop times (UTC) and synoptic description are given for each of 7 periods.

P	Date	Synoptic situation
1	1100 10 Jan - 2300 12 Jan	Easterly flow
2	2300 12 Jan - 1700 17 Jan	NE quad. of Aust. low
3	1700 17 Jan - 0500 23 Jan	W quad. of Irma
4	0500 23 Jan - 2300 28 Jan	Weak easterlies
5	2300 28 Jan - 1200 04 Feb	Westerly monsoon flow
6	1200 04 Feb - 2300 12 Feb	Cyclone Jason circ.
7	2300 12 Feb - 2300 14 Feb	Monsoonal westerlies

During Period 1, 10 - 12 January, easterly flow was present over Darwin. Fig. 1 shows daily totals of area-integrated radar-derived rainfall (kg) from the Darwin radar, and the convective and stratiform components of precipitation for each day. This analysis includes all radar echos except ground clutter near Darwin, and incorporates both

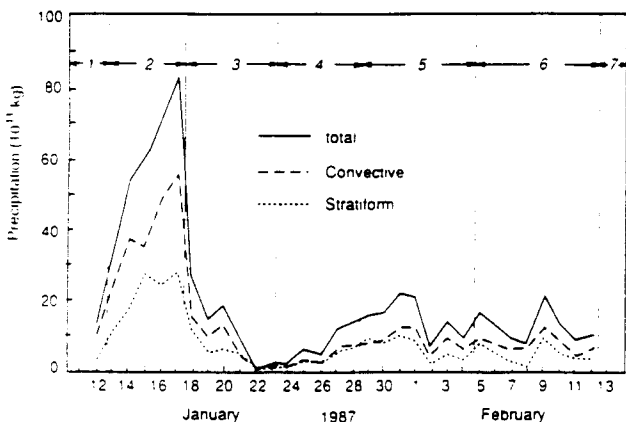


Figure 1: Area-integrated radar-derived precipitation (10^{11} kg) near Darwin. The solid line is the total precipitation; dashed is the convective component; and dotted is the stratiform component.

mesoscale systems and convective-scale precipitation. There was only one mesoscale system during the first period, and the precipitation near Darwin was associated mainly with isolated thundershowers. Since the radar at Darwin began recording data on 12 January, Period 1 was not well sampled by the radar data. However, satellite imagery showed that no mesoscale systems passed near Darwin on 10 and 11 January. Table 3 summarizes information on shear, stability, mean winds, and storm movement for the synoptic periods 1 through 7. Period 7 was not observed long enough by radar to sample any mesoscale systems.

Table 3: Wind and storm characteristics of each synoptic period. For each mesoscale system a pre-storm sounding was identified. The sounding parameters shown below are averages over all the pre-storm soundings in each of the six synoptic periods. Column N gives the number of mesoscale systems in each time period. The CAPE ($J kg^{-1}$) is the convective available potential energy for each period. SHEAR is the vertically averaged mass-weighted wind shear in the 0.5-to-6.0 km layer ($m s^{-1} km^{-1}$); SPEED is the rate of storm movement ($m s^{-1}$); DIR is the direction (deg) of storm displacement; and LL is the low-level wind speed (vertically averaged 700-to-900 mb wind speed). UL is the upper-level shear, represented by the magnitude ($m s^{-1}$) of the 100-to-400 mb wind vector difference.

P	N	CAPE	SHEAR	SPEED	DIR	LL	UL
1	1	2831	7.6	6	350	10	20
2	13	102	7.3	9	289	10	19
3	1	700	6.4	6	170	11	28
4	1	542	5.4	4	0	3	21
5	8	1774	4.7	13	268	15	29
6	8	1759	7.2	10	204	10	22
7	0	0	0	0	0	0	0

3.2 Period 2

During Period 2, westerly monsoonal flow from the ocean was present near Darwin, and a circulation center was located to the southwest. The area-integrated radar-derived precipitation (Fig. 1) was maximum, over half of the precipitation observed by the Darwin radar during EMEX fell, and 13 mesoscale systems occurred during this period. The precipitable water content (Fig. 2) increased from Period 1, and examination of time-height profiles of relative humidity (not shown) indicates that the moisture increase occurred primarily in the 400 - 600 mb layer. Hence, there was high relative humidity in the midlevel layers, and it appears that increases in midlevel humidity occurred simultaneously with the surge in precipitation.

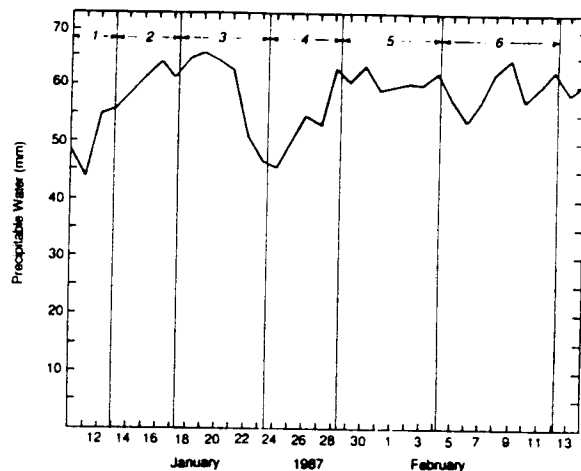


Figure 2: Precipitable water content (mm) at Darwin. Derived from 6-hourly soundings.

The systems during Period 2 generally had leading convective lines with well-developed trailing stratiform precipitation, were generally large (covered much of the radar domain), and moved at an average speed of $9 m s^{-1}$ from the west northwest. The lines generally moved by continuous propagation. The convective lines were generally perpendicular to the mean wind during Period 2, though one system was parallel. The convective component of the precipitation exceeded the stratiform component throughout this period.

Analysis of soundings indicated that the convective available potential energy (CAPE) for the pre-storm sounding of each of the lines observed at Darwin ranged from less than 1 to more than 4 kJ during EMEX, and that there was no systematic variation during the experiment.

The shear between 900 and 1000 mb (Fig. 3) was relatively high, and the west-east component of the wind during Period 2 was westerly throughout the troposphere (Fig. 4). Thus the monsoonal flow filled a deep layer. There was relatively little shear between the lower and upper troposphere. Time series of 700 to 900 mb wind shear (not shown) indicated no significant variation from period to period. Upper-tropospheric shear, however, varied greatly from period to period. Fig. 5 shows a time series of the magnitude of the wind-vector difference between 100 and 400 mb. During Period 2, the values averaged about $18 m s^{-1}$, which was much less than during Periods 3 and 5, but

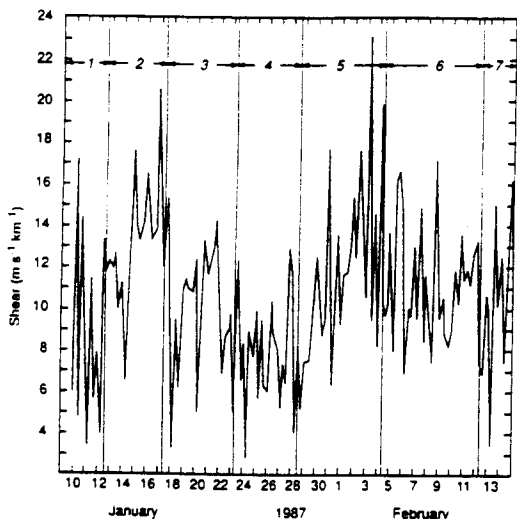


Figure 3: Time series of the magnitude of the wind shear vector between 900 and 1000 mb during EMEX. The synoptic scale periods 1 through 7 are labeled.

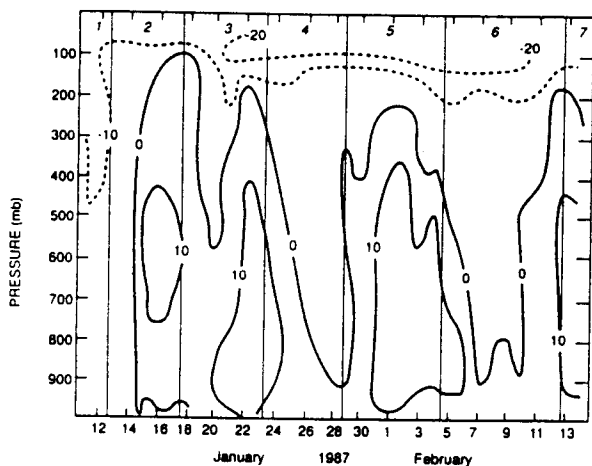


Figure 4: East-west component of wind as function of pressure and time. Solid lines are positive (westerly) winds labeled in $m s^{-1}$, and dashed lines are negative (easterly) winds.

comparable to 4 and 6. The relatively low shear at upper levels may have helped the stratiform precipitation areas to develop efficiently during this period by preventing the upper portion of the system from becoming dissociated with the lower portion.

The storm motion vectors during Period 2, as well as during the other active Periods 5 and 6 (discussed later), were close to the density-weighted 700-to-900 mb mean winds at the time of the storms. During Period 2, most of the storms moved at speeds of 8 to 14 $m s^{-1}$, and the ambient monsoon wind was 9 to 12 $m s^{-1}$. Most of the storms moved from 260 to 350°, while the 700-to-900 mb flow ranged from 300 to 350°. Periods 5 and 6 were similar, suggesting that the low-to-mid level flow acted as a steering current for the mesoscale systems.

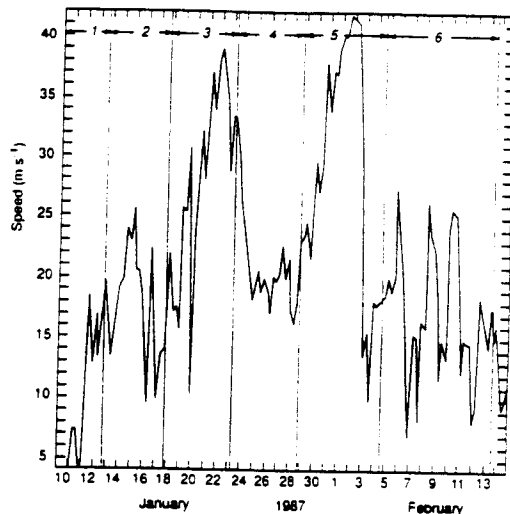


Figure 5: Time series of wind-shear vector magnitude between 100 and 400 mb.

An example of a mesoscale system from Period 2 is shown in Fig. 6. The infrared satellite image of the cloud-top temperature (Fig. 6a) shows a continuous cirrus shield, at a threshold temperature of 214 K, extending over 700 km.

Four pockets of lower cloud-top temperature, at a threshold of 196 K, are also shown, one of which was located over Darwin. The infrared data indicate that cloud temperatures were as low as 186° K, which suggests that cloud tops were reaching the tropopause at a pressure of about 90 mb. The corresponding Darwin sounding (not shown) indicated westerly winds extended from the top of the boundary layer to the tropopause. The radar-echo pattern (Fig. 6b) shows a large stratiform region of precipitation with a line of convective cells extending counterclockwise from 90 km east of Darwin to north and west of Darwin. Later more convective cells formed along this line and the line moved rapidly toward the northeast. The most intense convective cells were roughly collocated with the coldest cloud tops in the infrared image. Scattered convective cells were embedded in the stratiform region. It is evident from the satellite image that this system was much larger than the area surveyed by the Darwin radar; hence, much of the precipitation in this system was not observed by the ground-based radar. Although this system was perhaps the most intense one during EMEX, it was nonetheless typical of systems during the second period, which were characterized by large stratiform regions of precipitation, a moving line of intense convection, and scattered convection embedded in the stratiform region.

3.3 Period 3

During Period 3, beginning at 1700 UTC 17 January, Darwin was in the distant storm circulation of a tropical depression that formed over the Gulf of Carpentaria. This depression, which became cyclone *Irma*, indirectly influenced the weather at Darwin for several days. At 0000 UTC 20 January, Darwin was experiencing southwesterly winds at 700 mb on the west side of *Irma*. The amount of precipitation around Darwin decreased (Fig. 1) as the lower tropospheric winds shifted from northwesterly to southwesterly. The decrease in precipitation during this

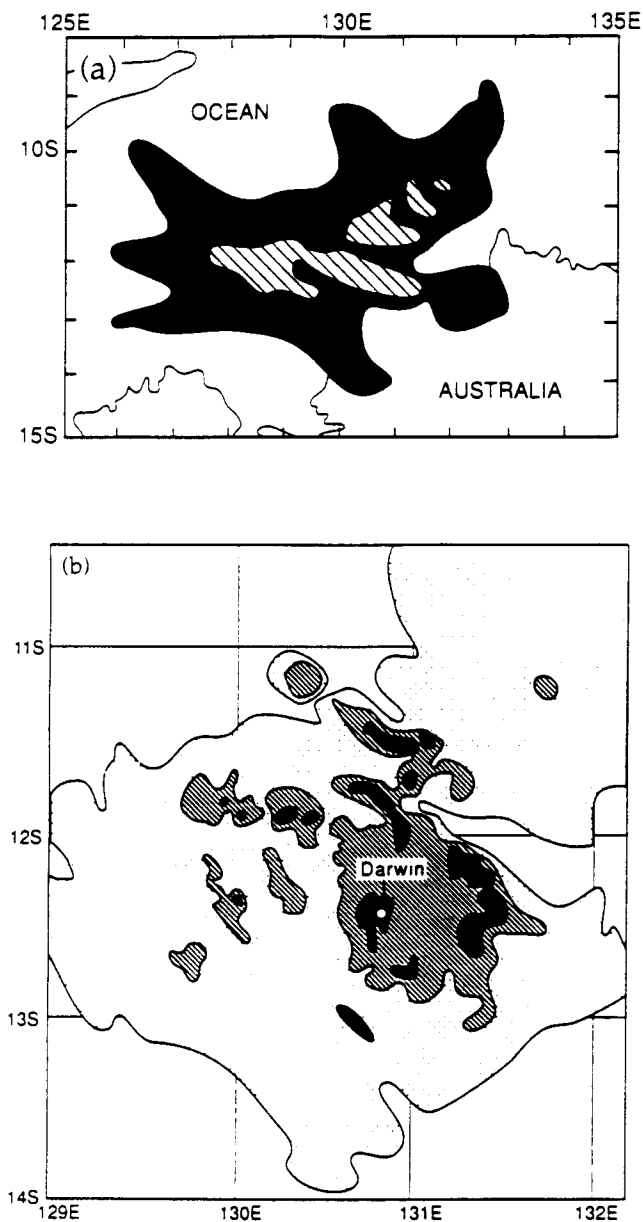


Figure 6: (a) Schematic diagram of blackbody temperatures from GMS-1 at 0250 UTC 15 January 1987. Shaded areas have temperatures in the range 197 to 214 K, hatched areas are 189 to 196 K. (b) Radar reflectivity from Darwin radar at 0301 UTC 15 January 1987. Hatched areas are 15 to 34 dBZ; cross-hatched areas are 34 to 42 dBZ; black areas are 43 dBZ and above.

period, despite the fact that the precipitable water content remained high during the first part of the period (Fig. 2), likely was due to subsidence in the environment west of the cyclone. The one mesoscale system, which occurred during this time, moved from the southwest and had a well-developed stratiform precipitation area.

During Period 4, from 23 to 28 January, Irma was dissipating south of Darwin, and winds at Darwin were westerly. At the beginning of this period, the precipitable water content was at a low of 36 mm (Fig. 2). Dry air from the continent had been advected over the region by the storm circulation. Darwin received no precipitation on 23 January, and the radar (Fig. 1) showed a minimal amount of precipitation near Darwin mostly associated with isolated convection. By the end of the period, the cyclone had dissipated completely and weak northerly winds and a circulation center had formed over the Bonaparte Gulf southwest of Darwin. Weak northerly winds had increased the precipitable water to 60 - 70 mm and the areal rainfall had increased (Fig. 1). The u-component of the wind remained near zero throughout the low-to-upper troposphere during 24 to 27 January (Fig. 4), the boundary-layer shear was weak (Fig. 3), and the upper-level shear was moderate (Fig. 5).

Only one mesoscale system formed during Period 4 (Tables 2 and 3), and it was characterized by convection embedded in stratiform precipitation, with no line orientation to the convection, and no clear direction of movement. Fig. 1 shows that nearly equal amounts of stratiform and convective precipitation were evident in the radar data during Period 4, in contrast to other periods, when convection accounted for the majority of the rainfall. The amorphous structure may have been because of a lack of low-level shear that is needed for convective lines to form. The moderate upper-level shear evidently allowed local areas of stratiform precipitation to form surrounding the convection.

3.5 Period 5

By 2300 UTC 1 February, the flow over Darwin was no longer affected by the cyclonic circulation to the south, and the 700 mb wind speed had increased to 15 m s^{-1} from the west. Throughout Period 5, the precipitable water content was in the range 55 - 60 mm, and moderate amounts of precipitation were observed by radar (Fig. 1). During most of this period, the convective rainfall slightly exceeded the stratiform component. The 8 mesoscale systems observed on radar during the period moved from the west at a mean speed of 13 m s^{-1} , which was faster than the systems observed during Period 2. On radar, these systems generally comprised a narrow (about 10 km wide) band of convective cells, often poorly aligned or twisted, which appeared to meander or wiggle as the system moved through the area of radar coverage. These systems generally had poorly formed or non-existent stratiform rain regions behind them on radar. However, there was much scattered stratiform precipitation seen in the radar data that was not clearly associated with any convective line. These areas of stratiform precipitation were apparently the dissipating remnants of convection that advected into the range of the radar.

The u-component of the wind was westerly at 15 m s^{-1} in a deep layer from the surface to about 300 mb, but above that winds were easterly up to 20 m s^{-1} near 100 mb (Fig. 4). This produced high shear between the middle

and upper levels during Period 5 (Fig. 5). Radar images viewed in a time-lapse movie sequence and animated computer displays of infrared satellite image, suggested that the stratiform precipitation was associated with cloud and precipitation particles that were being rapidly moved westward relative to the convective lines. The infrared and visible satellite images of the clouds in this region had a very streaky appearance, with the streaks being roughly aligned with the 700 mb wind vectors. Hence we believe that while strong boundary-layer shear (Fig. 3) was conducive for convective line formation, high upper-level shear led to fractured, poorly formed, or non-existent stratiform regions.

An example of such a system is shown in Fig. 7. Panel a shows the infrared cloud-top temperatures. A cloud shield about 300 km in length was located over Darwin, while a much larger system, centered at about 11 S, 134 E, was out of range of the Darwin radar. The radar pattern for this system (Fig. 7b) shows two convective lines. The first was oriented northwest to southeast and was about 300 km long, closely matching the orientation and length of the cirrus shield seen in the infrared. This line moved toward the east at about 17 m s^{-1} . The convection in this line had cloud-top temperatures no lower than 204 K, which corresponds to about 150 mb; hence this convection was not reaching the tropopause. The stratiform precipitation was only about 50 km wide behind the convective line. The lack of extensive stratiform precipitation suggests that no mesoscale updraft was present behind this line, and there likely was no mesoscale downdraft either, since there was too little precipitation to melt, evaporate, and promote the subsidence identified with mesoscale downdrafts (Zipser, 1977). The soundings for this case did not indicate a mesoscale downdraft was present. The second convective line was located west of Darwin, and had the same velocity as the larger convective line. This line was very narrow, had weaker convection, and was devoid of stratiform precipitation.

The presence of two lines so close to each other further suggests that the convection in the leading line did not exhaust the boundary layer of its moisture, nor did it suppress the boundary layer, as mesoscale downdrafts tend to; hence, the environmental conditions remained suitable for a second line form in the wake of the first line. The soundings in this case differed little from the 15 January case, except that the upper tropospheric winds, above about 300 mb, were strongly from the east. Stratiform precipitation regions evidently could not form well because of the upper level shear. Recent studies have emphasized the importance of low-level shear in the formation of squall lines with trailing stratiform precipitation (Weisman et al., 1988; Fovell and Ogura, 1988, 1989), the differences in mesoscale structure between Periods 2 and 5 suggest that the upper-level shear also affects mesoscale organization.

3.6 Period 6

During Period 6, from 4 - 12 February, the wind flow at Darwin was influenced by another cyclone, *Jason*, which formed over the Gulf of Carpentaria. During this period the rainfall amounts in Darwin and vicinity were variable but moderate (Fig. 1), and winds varied in direction. The precipitable water content fluctuated as the

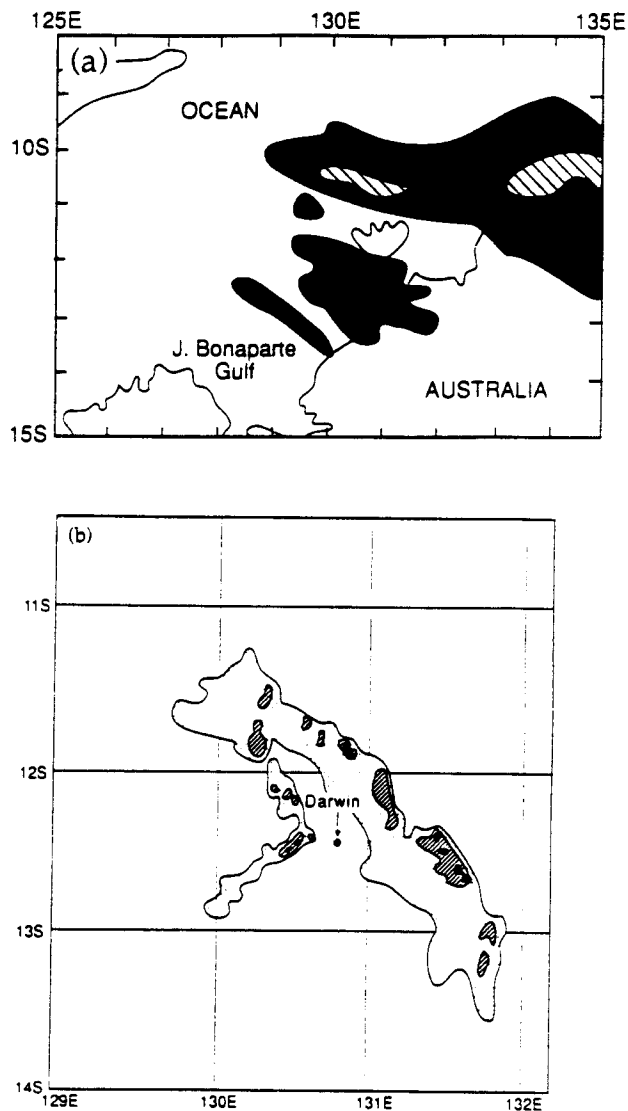


Figure 7: (a) Schematic diagram of blackbody temperatures from GMS-1 at 0300 UTC 1 February 1987. Shaded areas have temperatures in the range 197 to 214° K; hatched areas are 189 to 196° K. (b) Radar reflectivity from Darwin radar at 0220 UTC 1 February 1987. Hatched areas are 15 to 34 dBZ; cross-hatched areas are 34 to 42 dBZ; black areas are 43 dBZ and above.

wind alternately advected air from marine and continental sources, but remained fairly high throughout the period. The upper-level shear (Fig. 5) was comparable to Period 2, and the boundary-layer shear (Fig. 3) was about the same as during Period 2 (Table 3). The systems during Period 6 came from the southwest at an average speed of 10 m s^{-1} , in close agreement with the 700-to-900 mb wind during this period. These systems had well-developed stratiform regions and convective lines and were about as intense as those observed during Period 2.

During the final Period 7, the wind flow over Darwin returned to monsoonal westerlies. The experiment ended before any mesoscale systems were observed during Period 7.

4. SUMMARY AND CONCLUSIONS

The mesoscale and synoptic-scale conditions near Darwin during the Australian Mesoscale Experiment have been examined using land-based radar, rain gauge, soundings, and satellite measurements. Within synoptic-scale time periods of 3 to 8 days, during which the wind and humidity structures of the atmosphere were similar, there was a noteworthy consistency in the structure and organization of mesoscale systems. In general, mesoscale systems were not present when precipitable water content was below about 50 mm, or when convective activity appeared to be suppressed in the synoptic-scale vicinity of tropical cyclones. Periods of high precipitable water content were generally cotemporous with observations of mesoscale systems.

The dominant synoptic-scale parameters related to mesoscale system characteristics were boundary-layer shear, the mean wind in the 700-to-900 mb layer, and shear in the 100-to-400 mb layer. Low wind speeds (less than 5 m s^{-1}) in the 700-to-900 mb layer accompanied by low boundary-layer shear, in the presence of low-level forcing associated with a circulation center, favored scattered convection embedded in stratiform precipitation, and nearly equal amounts of convective and stratiform precipitation. When boundary layer shear was greater than about $10 \text{ m s}^{-1} \text{ km}^{-1}$, line-oriented convection developed, and the convective component of precipitation exceeded the stratiform component. When upper-level shear (represented by the 100-to-400 mb wind shear vector) was less than about 25 m s^{-1} well developed stratiform rain areas were present behind the convective lines; but when the upper-level shear increased in magnitude to 30 to 40 m s^{-1} , the stratiform regions were fragmented or poorly formed. The 700-to-900 mb wind acted as a steering current for the mesoscale systems, i.e. nearly all the storms had displacement vectors commensurate with this wind vector. Faster moving systems apparently did not perturb the boundary layer much, as they were often followed by other lines with less than about 100 km between them.

These results suggest that the mesoscale structure and organization of convection near Darwin during EMEX were consistent within the context of synoptic-scale weather conditions, and suggest that the diabatic heating of mesoscale convection on synoptic time scales could possibly be parameterized for use in numerical weather prediction or general circulation models. However, the high degree of variability in structure and organization from one synoptic region to another suggests that the diabatic heating associated with the convection likely varies significantly from one synoptic-scale setting to the next.

5. ACKNOWLEDGEMENT

EMEX data were generously provided to us by the Australian Bureau of Meteorology. R. M. Zehr of Colorado State University helped us obtain the infrared and visible GMS-1 satellite imagery. The authors benefitted from many interesting discussions with Brian Mapes during this study, and G. C. Gudmundson edited the manuscript. K. Dewar drafted the figures. Funding for this research was provided by NASA grant NAG 5-784, and the National Science Foundation, grant ATM8616647.

REFERENCES

- Churchill, D. D. and R. A. Houze, Jr., 1984: Development and structure of winter monsoon cloud clusters on 10 December 1978. *J. Atmos. Sci.*, **41**, 933 - 960.
- , and —————, 1991: Mesoscale convective systems and large-scale flow near Darwin Australia during the Australian Monsoon Experiment. Submitted to *Mon. Wea. Rev.*.
- Fovell, R. G., and Y. Ogura, 1988: Numerical simulation of a midlatitude squall line in two dimensions. *J. Atmos. Sci.*, **45**, 3846 - 3879.
- , and —————, 1989: Effects of vertical wind shear on numerically simulated multicell storm structure. *J. Atmos. Sci.*, **46**, 3144 - 3176.
- Weisman, M. L., J. B. Klemp and R. Rotunno, 1988: A theory for strong, long-lived squall lines. *J. Atmos. Sci.*, **45**, 463 - 485.
- Zipser, E. J., 1977: Mesoscale and convective-scale downdrafts as distinct components of squall-line circulation. *Mon. Wea. Rev.*, **105**, 1568 - 1589.